
Original Research Article

**SPRAY-DRIED, BIODEGRADABLE, Linezolid-LOADED
MICROSPHERES FOR USE IN THE TREATMENT OF LUNG
DISEASES**

ABSTRACT

Background: Researchers worldwide are currently seeking innovative treatment options to combat the alarming increase in bacterial resistance to antimicrobial drugs. Staphylococcus aureus, a frequently encountered and potentially life-threatening bacterium, has become particularly problematic. Linezolid is one of the few medicines on the market that can treat bacteria resistant to other antibiotics. This is the first antibacterial oxazolidinone that has shown to be therapeutically efficacious. Linezolid is a new Oxazolidinone medicine. It kills a broad spectrum of bacteria, including Staphylococcus aureus. **Objectives:** To reduce non-target organ adverse effects associated with frequent and chronic Linezolid usage, we developed biodegradable, lung-targeted microspheres with sustained release profile. **Methods:** In this work, a Buchi B-90 nanospray drier was used to prepare a Linezolid-loaded carbopol microsphere (CLSMO)-based formulation. The spray-drying process was optimized using a face-centered central composite design (CCD). **Results:** The average particle size was 7.516 μm , and the surface of the microspheres was shriveled, according to scanning electron microscope imaging. Drug content and yield were determined to be 73% 3.1% and 72% \pm 2.4%. , respectively, and drug release (99.1%) peaked for up to 12 hours in vitro. FTIR spectral analysis results suggest that there are no significant physical and chemical interactions between the functional groups of Linezolid and carbopol 934P polymer which ultimately form a stable blend. Linezolid, Carbopol, and CLSMO all had XRD patterns that showed the linezolid would be molecularly dispersed in the polymer. The DSC

findings revealed the drug's amorphous nature, which explains the absence of characteristic peaks, indicating a lack of well-defined crystalline structure. **Conclusion:** The optimized formulation shows significant potential for use as a drug-delivery system in in-vivo applications, particularly in targeted drug delivery to the lungs

UNDER PEER REVIEW

INTRODUCTION

1.1. Introduction

Drug delivery is the process of delivering a medication or other pharmacologically active substance to a target cell in order to treat a condition or health problem. Drug delivery can take place by oral or intravenous or rectal, intranasal, intramuscular, transdermal, subcutaneous, pulmonary, or buccal. However, these methods have certain drawbacks, for example instability, side effects, uncontrolled release, slow absorption, and enzymatic degradation. To address these issues, targeted drug delivery (TDD) has been developed.

Microspheres are used for delivery of drugs to a particular target site because of its properties as its size is tiny, its shape is spherical and it is biodegradable particles. It offers enhanced drug loading capabilities and can be designed to provide specific release profiles and target specific tissue sites. Not only that but also it can be engineered to possess certain desirable characteristics like sustained or controlled release, improved drug solubility, and increased drug stability. Drugs which are sensitive to temperature or PH or light and different types of drugs can be used with microspheres.

Research Aim and Objectiv

The aim of this study is to develop and characterize microspheres containing linezolid for lung delivery, with the particle size ranging from 5-15 microns by intravenous route.

METHODOLOGY

3.1. Formulation Studies

Spray drying is a typical method for preparing microspheres for drug delivery applications. It has been used to manufacture a variety of drug delivery systems, like microspheres, nanocomposites, nanospheres, and liposomes. It is an easy, flexible, and affordable approach.

3.2 Optimization

There are some variables affect how well a product turns out after being spray-dried these variables may be critical process variables or formulation variables or both. Thus, the transfer of this technology from the laboratory scale to the production plant is significantly speed up by using the quality by design (QbD) method in conjunction with process analytical technology (PAT). The relationships between them in such a procedure are complicated and occasionally challenging to predict because there are many parameters that may be manipulated.

Procedure

Carbopol microspheres containing linezolid were prepared using the Buchi Nano Spray Dryer technique with the carbopol concentration (100mg–500 mg), inlet temperature (80°C–100°C) and flow rate (20–25 mL/h). 1:1 solutions of carbopol and linezolid were prepared in 100 mL of water, warmed to 25°C, with a viscosity 15 cP (centipoise) suitable for spraying through the nozzle. The dispersion was then fed through a 7 mm nozzle and the outlet temperature was kept in the range of 30°C–50°C. All samples were filtered prior to spray drying in order to prevent nozzle blockage. The dried particles were collected manually with a particle scraper and stored in desiccators at room temperature for further examination.

3.3. Estimation of pure drug linezolid

Estimation of linezolid in microspheres involves the preparation of a standard solution of linezolid by dissolving an accurately weighed quantity of the drug in a methanol, then preparation of a series of dilutions by diluting the standard solution with the same solvent. The absorbance of each solution is measured using an UV-visible spectrophotometer at a wavelength of λ_{\max} of linezolid, which is 284 nm.

3.4. Percentage Recovery/ Yield

The percentage weight of the resulting microspheres was used to calculate the spray-dried small particle recovery, which was compared to the initial amounts of carbopol and linezolid utilized in the formulation process, and this percentage can be calculated by the following equation

Equation 1: Microsphere recovery

Microspheres recovery

$$= \frac{\text{Recovered Weight of Microspheres}}{\text{Weight of the polymer used} + \text{Drug}} \times 100$$

3.5. Drug loading in microsphere

Drug loading is the amount of drug in a formulation, it is expressed as a percentage of the formulation's overall weight.

A solvent extraction approach was employed to determine the drug loading of linezolid in spray dried microspheres. At first the microspheres are homogenized in an acetonitrile solution. Then the filtrate is collected by filtration of the homogenized solution. The amount of drug in the filtrate is then measured using linezolid's UV spectrophotometry at 284 nm in wavelength. Finally, the drug loading is then determined by dividing the drug concentration in the filtrate by the sum of the microspheres' weight using the following equation.

Equation 2: drug loading

$$\% \text{ Drug Loading} = \frac{\text{Quantity of Linezolid present}}{\text{Microspheres}} \times 100$$

3.6. Surface Morphology Procedure

The powders were imaged by a scanning electron microscope (SEM) run at an accelerating voltage of 10kV using Hitachi SU 3500. The powder in few µg were fixed on to stub by a double sided sticky carbon tape and kept inside the SEM chamber and analyzed at different magnification like 60X, 200X, 500X, 1.10X and 2.50X respectively to obtain better clarity on the particle morphology/ topology.

3.7. Particle Size Measurement

The Particle Size distribution of a 10 milligram sample obtained from a spray dryer was determined using a Malvern Zetasizer Nano ZS (Malvern Instruments, Malvern, UK). The sample was suspended in 10 mL of an organic

solvent and ultrasonicated, then added three-quarters full to a reusable glass cuvette. The distribution was measured by taking three readings and averaging the results

3.8. Differential Scanning Calorimetry (DSC)

Differential Scanning Calorimetry (DSC) is a thermo analytical technique in which the difference in the amount of heat required to increase the temperature of a sample and reference are measured as a function of temperature. Both the sample and reference are maintained at nearly the same temperature throughout the experiment.

Procedure

DSC (Perkin-Elmer- 4000 series) experiments were carried out in order to characterize the physical state of the drugs. Samples of formulation were placed in aluminium pans and thermally sealed. The heating rate was 20°C per minute using nitrogen as the purge gas. The DSC instrument was calibrated for temperature using Indium. In addition, for enthalpy calibration Indium was sealed in aluminium pans with sealed empty pan as a reference.

3.9. X-ray diffraction analysis (XRD)

XRD analysis, is a technique used in materials science to study of the crystal structure, it is used to identify the crystalline phases present in a material and thereby reveal chemical composition information.

3-10 Fourier transform infrared spectrometry (FTIR)

Procedure: Infrared spectra of samples were recorded in Bruker ATR alpha kept at an ambient temperature of $25.0 \pm 0.5^\circ\text{C}$. The analytical procedure was simple and did not need any special sample preparation. The spectra were recorded by placing the samples on a zinc selenoid crystal plate and screwing the anvil over the sample carefully and scanning. The samples in region of $4000\text{-}400\text{ cm}^{-1}$ to determine various functional groups. The IR spectra of the samples was checked for any possible drug excipients interaction

3.10. In vitro release studies

Release studies are key components in the development of conventional drug delivery systems and novel drug delivery formulations. These studies are important in determining the optimal release rate of the drug from the delivery system, as well as its effectiveness in targeting the desired site of action.

Procedure:

predetermined time intervals to measure the drug content which was determined at 252 nm using a UV-VIS spectrophotometer (1601; Shimadzu Corporation). The data obtained from the studies were analyzed using Sigma plot software version 12.0.3.0 (Systat Software, Inc., San Jose, CA, USA) and different kinetic models were used to understand the release mechanism. The experiment was conducted in triplicate (mean \pm SD, n=3). The obtained data were fitted to different kinetic models to understand the release mechanism using Sigmaplot software version 14.5 (Systat Software, Inc., San Jose, CA, USA).

RESULTS AND DISCUSSION

4.1. Optimization

The results of particle size optimization were fitted to a quadratic regression model, resulting in the maximum values of R² and model sum of squares. Analysis of variance (ANOVA) was performed on the results, and showed that the model was statistically significant.

4.2. Experimental Design Methodology

An experimental design methodology was employed to prepare batches of linezolid, with the aim of obtaining a desired particle size range (between 5–15 μm). A rotatable central composite design was chosen to investigate the effects of three operating variables (concentration of polymer, feed flow rate, and rotation speed) on the particle size of the microspheres, and the results of the experiment were analyzed using the Stat-Ease software.

Table 1. Software and Experimental Design

File Version	12.0.3.0		
Study Type	Response Surface	Subtype	Randomized
Design Type	Central Composite	Runs	15
Design Model	Quadratic	Blocks	No Blocks
Build Time (ms)	5.00		

Table 2 Experimental plan for linezolid microspheres

Name	Units	Type	Low	High
Carbopol Conc	mg	Factor	100	500
Intel Temp	DC	Factor	80	100
Feed Flow	ml	Factor	20	25
Particle size	nm	Response	5980	9004

Table 3 Experimental Design Layout

		Factor 1	Factor 2	Factor 3	Response 1
Std	Run	A:Carbopol Conc	B:Intel Temp	C:Feed Flow	Particle size
		Mg	DC	ml	Nm
15	1	300	90	23	7200
9	2	300	90	19	6400
11	3	300	90	23	7350
14	4	300	90	23	7125
12	5	300	90	23	7300
3	6	100	100	25	7130
4	7	100	80	20	6368
7	8	300	76	23	8875
13	9	300	90	23	7115
10	10	300	90	26	8315
5	11	17	90	23	5980
1	12	500	100	20	7884
8	13	300	104	23	6265
6	14	583	90	23	8395
2	15	500	80	25	9004

4.3 Estimation of pure drug linezolid

After that a calibration curve is plotted as X-axis was the concentration of the standard solution, and Y-axis was the absorbance of the respective solution, this calibration curve is used to calculate the concentration of linezolid in the test solution. An aliquot of the test solution is taken and its absorbance is measured using the UV-visible spectrophotometer at the same

wavelength of λ_{max} of linezolid and using the calibration curve, the concentration of linezolid in the test solution is determined.

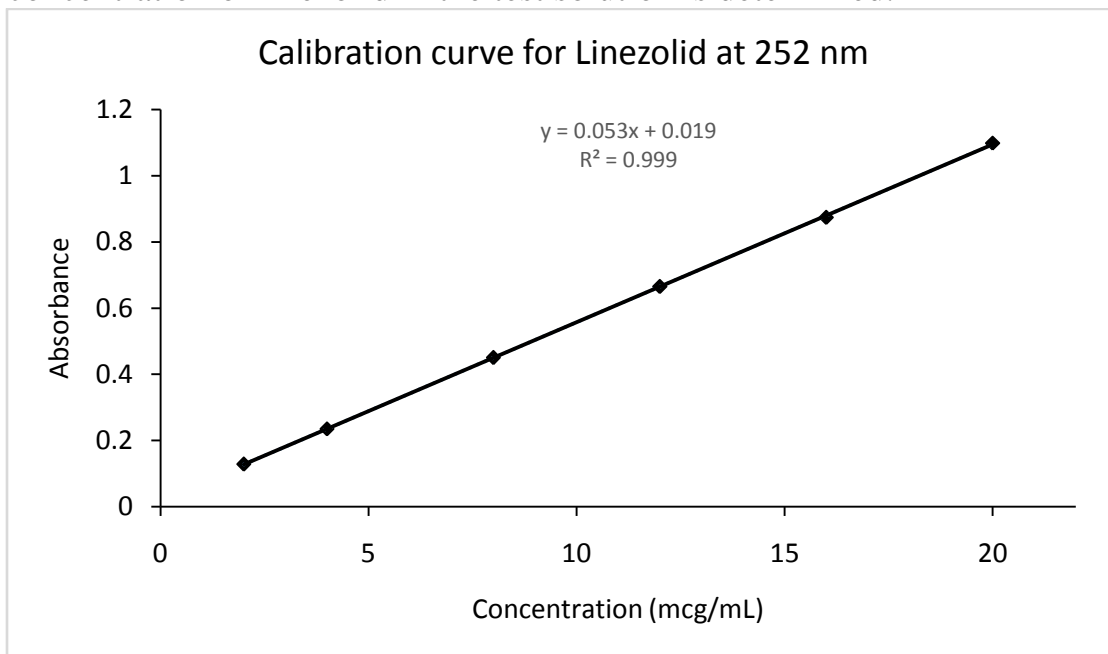


Figure 1 : calibration curve of linezolid at 252nm

4.4 Drug Loading and Yield

The particle yield for a CLSMO-1 formulation was computed to be 72% \pm 2.4%. During the drying process, some of the product was found to bind to the electrostatic particle collector and electrodes, which was likely caused by the low density of the particles formed after drying. To reduce this issue, it is suggested to increase the volume of liquid delivered into the drying chamber; however, some of the product will still be lost. The drug content of the same formulation was found to be 73% 3.1%.

The particle yield for a CLSMO-1 formulation was calculated to be 72% \pm 2.4%. During the drying process, some of the particles was appeared to stick to the electrostatic particle collector and electrodes, which was most likely caused by the low density of the particles formed after drying. To address this issue, it is proposed that the volume of liquid fed into the drying chamber be increased; however, some particles will still be lost. The drug content of the identical formulation was found to be 73% 3.1%.

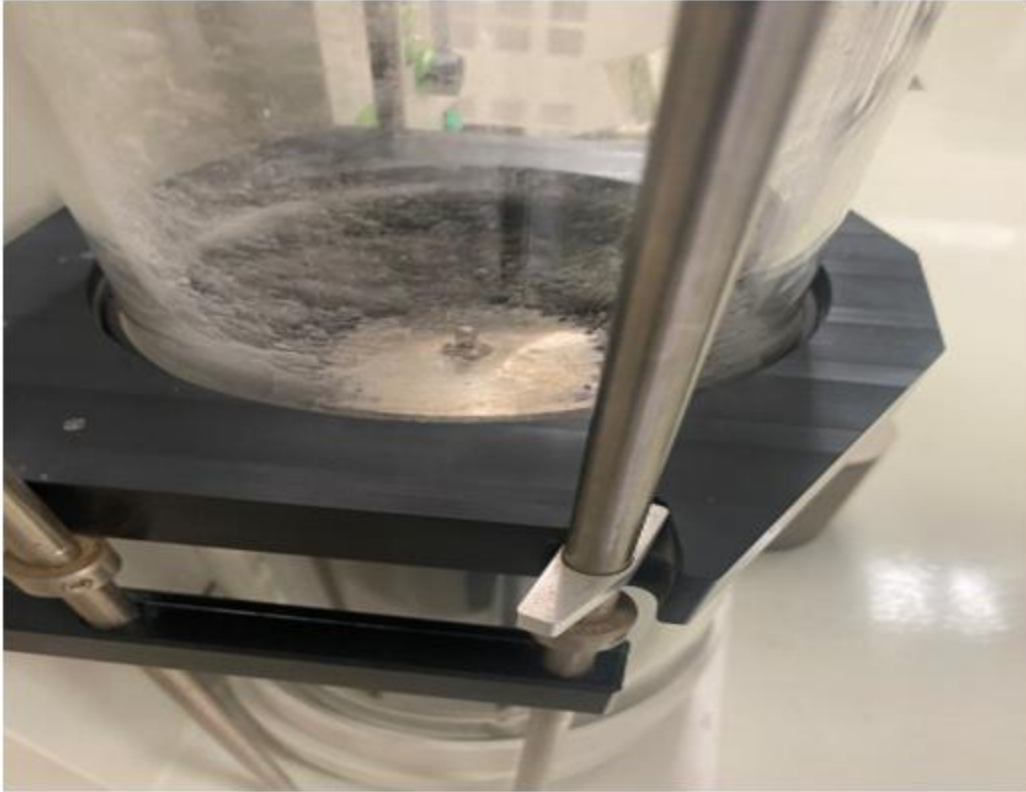


Figure 2: Buchi Spray Dryer Glass Chamber showing particle sticking



Figure 3: Buchi Spray Dryer Particle Collector showing particle sticking

4.5.Surface Morphology

There are three main reasons that make the importance of surface morphology studies for drug formulation. The first reason is: they provide information on the physical characteristics of a drug product. This information is essential for understanding the properties of the drug product, like its size, surface area, shape, porosity, and crystallinity. The second reason is: They can provide insight into the manufacturing process of a drug product, including particle size distribution and homogeneity which can help to optimize the manufacturing process and ensure that the drug product is of a consistent quality. The third reason is: They can help identify potential issues with a drug product, such as non-uniformity, particle agglomeration, or contamination which can be used to improve the quality of the drug product and reduce the risk of adverse events.

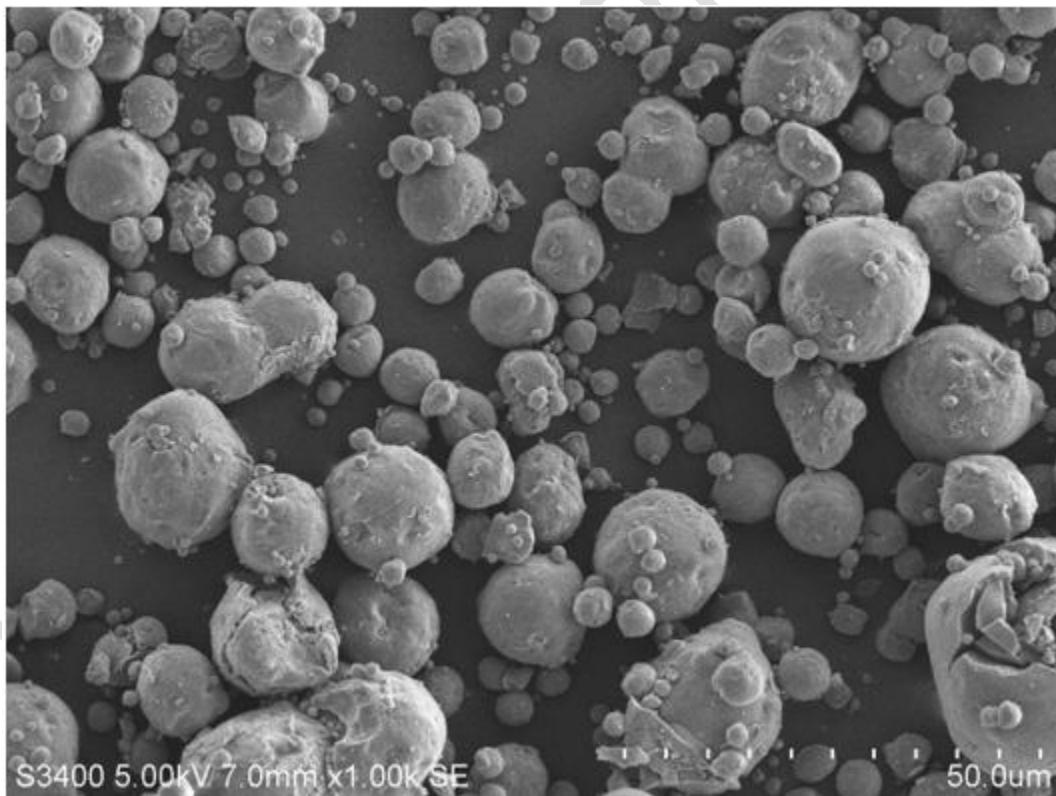


Figure 4: Spray dried Surface Morphology of CLSMO-1

4.6.Particle Size Analysis

Particle size analysis is an important tool for optimizing targeted drug delivery to the lungs via the intravenous route by microspheres entrapped in the capillary network of the lungs. particle size analysis can help to ensure

that drugs are delivered to the lungs in an effective and safe manner by providing detailed information on the size and shape of the particles, as well as the efficiency of the delivery system.

The particle size of Carbopol microspheres containing linezolid was observed to be a key parameter for drug delivery. This particle size is in the optimal range of 5 - 15 μm , which is necessary for particle entering the lung tissue. Particle size also plays a significant role in targeting the particles to a specific region of the lung. The experimental data point showed a particle size of 7.302 μm , which is suitable for lung targeting.

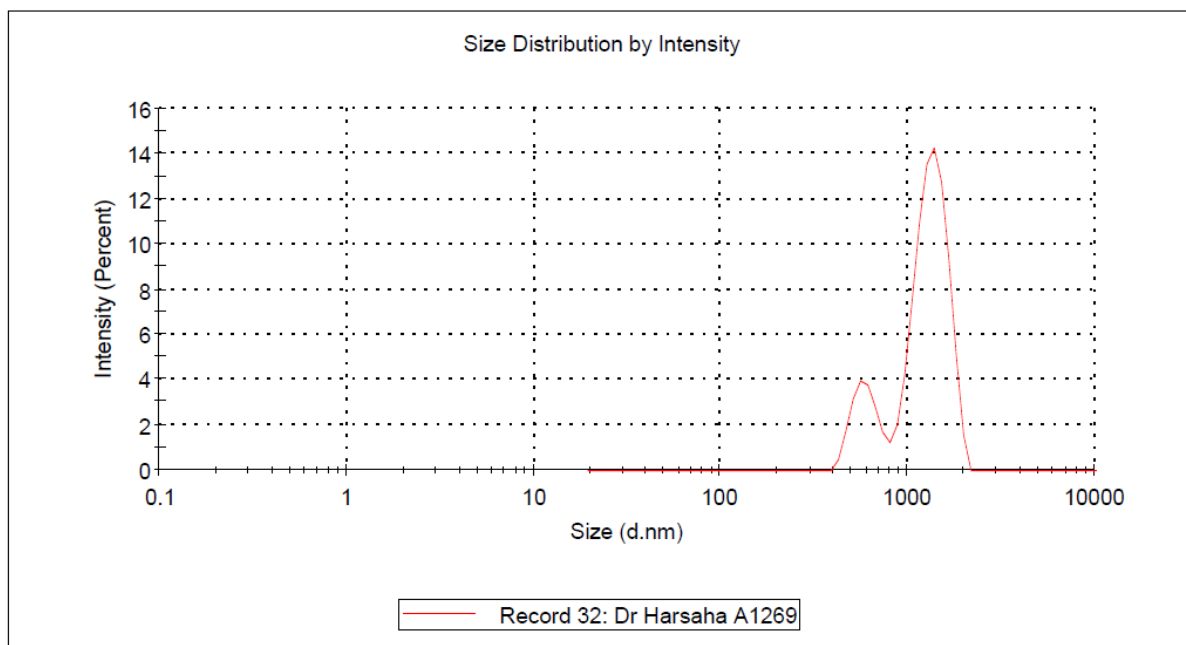


Figure 5: particle size analysis of Carbopol microspheres containing linezolid

Table 4 Results of Experimental Design Table for three factors

		Factor 1	Factor 2	Factor 3	Response 1
Std	Run	A:Carbopol Conc	B:Intel Temp	C:Feed Flow	Particle size
		mg	DC	MI	Nm
15	1	300	90	23	7200
9	2	300	90	19	6400
11	3	300	90	23	7350
14	4	300	90	23	7125
12	5	300	90	23	7300
3	6	100	100	25	7130
4	7	100	80	20	6368

7	8	300	76	23	8875
13	9	300	90	23	7115
10	10	300	90	26	8315
5	11	17	90	23	5980
1	12	500	100	20	7884
8	13	300	104	23	6265
6	14	583	90	23	8395
2	15	500	80	25	9004

Response 1: Particle size

Table 5 ANOVA for Quadratic model

Source	Sum of Squares	df	Mean Square	F-value	p-value	
Model	1.238E+07	9	1.376E+06	90.28	< 0.0001	significant
A-Carbopol Conc	2.916E+06	1	2.916E+06	191.40	< 0.0001	
B-Intel Temp	3.406E+06	1	3.406E+06	223.55	< 0.0001	
C-Feed Flow	1.834E+06	1	1.834E+06	120.35	0.0001	
AB	85329.72	1	85329.72	5.60	0.0642	
AC	1.389E+06	1	1.389E+06	91.15	0.0002	
BC	80.17	1	80.17	0.0053	0.9450	
A ²	4123.68	1	4123.68	0.2707	0.6251	
B ²	3.545E+05	1	3.545E+05	23.27	0.0048	
C ²	90180.11	1	90180.11	5.92	0.0592	
Residual	76180.37	5	15236.07			
Lack of Fit	32450.37	1	32450.37	2.97	0.1600	not significant
Pure Error	43730.00	4	10932.50			
Cor Total	1.246E+07	14				

Factor coding is **Coded**.

Sum of squares is **Type III – Partial**

The Model F-value of 90.28 implies the model is significant. There is only a 0.01% chance that an F-value this large could occur due to noise.

P-values less than 0.0500 indicate model terms are significant. In this case A, B, C, AC, B² are significant model terms. Values greater than 0.1000 indicate the model terms are not significant. If there are many insignificant model terms (not counting those required to support hierarchy), model reduction may improve the model.

The **Lack of Fit F-value** of 2.97 implies the Lack of Fit is not significant relative to the pure error. There is a 16.00% chance that a Lack of Fit F-value this large could occur due to noise. Non-significant lack of fit is good - - we want the model to fit.

Table 6: Fit Statistics

Std. Dev.	123.43	R²	0.9939
Mean	7380.40	Adjusted R²	0.9829
C.V. %	1.67	Predicted R²	0.7131
		Adeq Precision	28.9170

The **Predicted R²** of 0.7131 is not as close to the **Adjusted R²** of 0.9829 as one might normally expect; i.e. the difference is more than 0.2. This may indicate a large block effect or a possible problem with the model and/or data. Things to consider are model reduction, response transformation, outliers, etc. All empirical models should be tested by doing confirmation runs.

Adeq Precision measures the signal to noise ratio. A ratio greater than 4 is desirable. The ratio of 28.917 indicates an adequate signal. This model can be used to navigate the design space.

Table 7: Final Equation in Terms of Actual Factors

Particle size	=
+26352.70602	
+32.12473	Carbopol Conc
-514.82561	Intel Temp
-30.47334	Feed Flow
+0.103277	Carbopol Conc * Intel Temp
-1.66655	Carbopol Conc * Feed Flow
+0.253258	Intel Temp * Feed Flow
+0.000578	Carbopol Conc ²

+2.14370	Intel Temp ²
+17.29926	Feed Flow ²

The equation in terms of actual factors can be used to make predictions about the response for given levels of each factor. Here, the levels should be specified in the original units for each factor. This equation should not be used to determine the relative impact of each factor because the coefficients are scaled to accommodate the units of each factor and the intercept is not at the center of the design space.

Particle size

Color points by value of

Particle size:

5980  9004

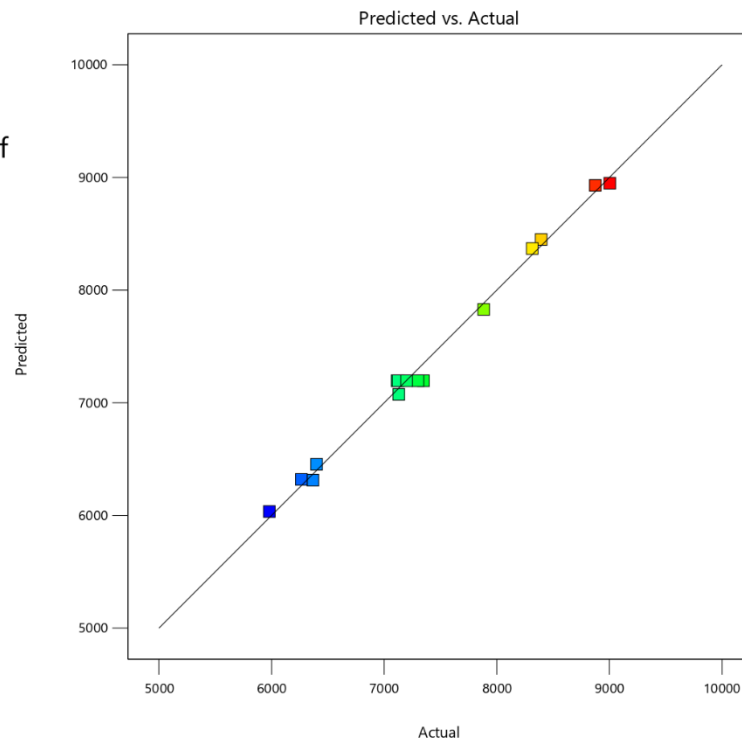


Figure 6: Predicted vs. Actual

The linear pattern observed in the predicted vs. actual values of particle size shows that the observed responses were in good correlation with the predicted one.

Particle size

Color points by value of Particle size:

5980  9004

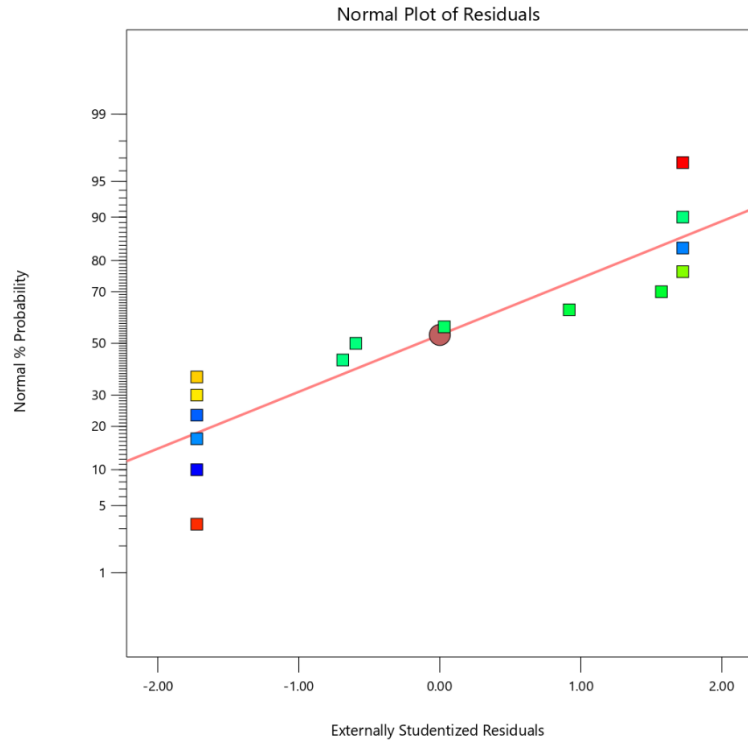
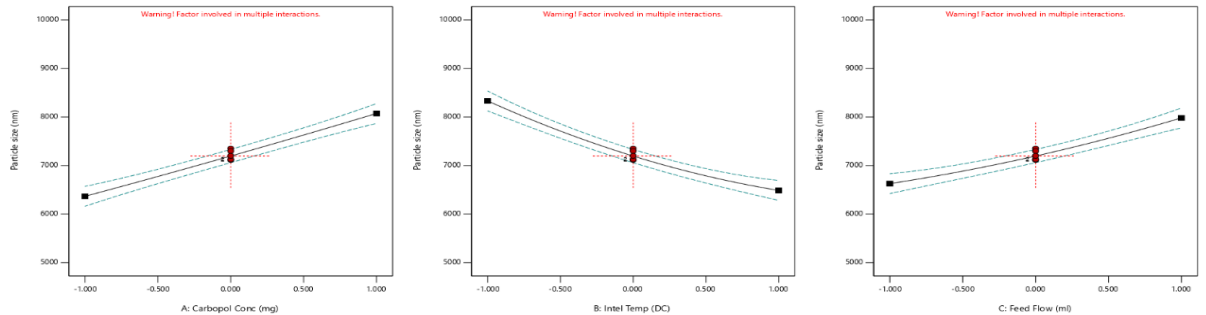


Figure 7: Normal Plot

The normal probability plot of the residuals suggests that the error terms are normally distributed.

Factor Coding: Coded
 Particle size (mm)
 ● Design Points
 --- 95% CI Bands
 Coded Factors
 A = 0.000
 B = 0.000
 C = 0.000



Positive correlation between Carbopol Conc and particle size.

Negative correlation between Intel Temp and particle size.

Positive correlation between Feed Flow and particle size.

Figure 8 Factors effects

From the previous figure there are: Positive correlation between particle size and both Carbopol Conc and Feed Flow, but negative correlation between Intel Temp and particle size.

Interpretation:

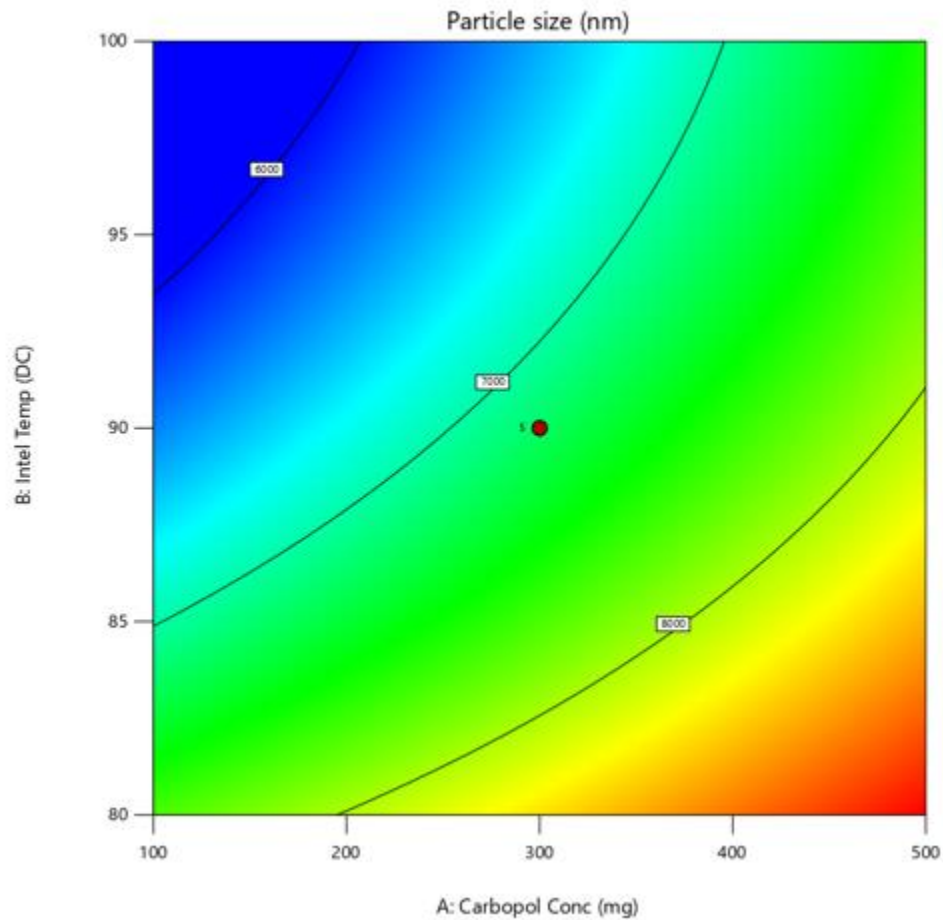


Figure 9: Contour Plots (2D) particle size, intel temp., and Carbopol conc.

From the previous figure it is noticed when the Carbopol Conc reached 500mg, big size particles were observed with temperature between 80°C to 85°C. As temperature increases in spray-drying preparation, the size of the particles decreases.

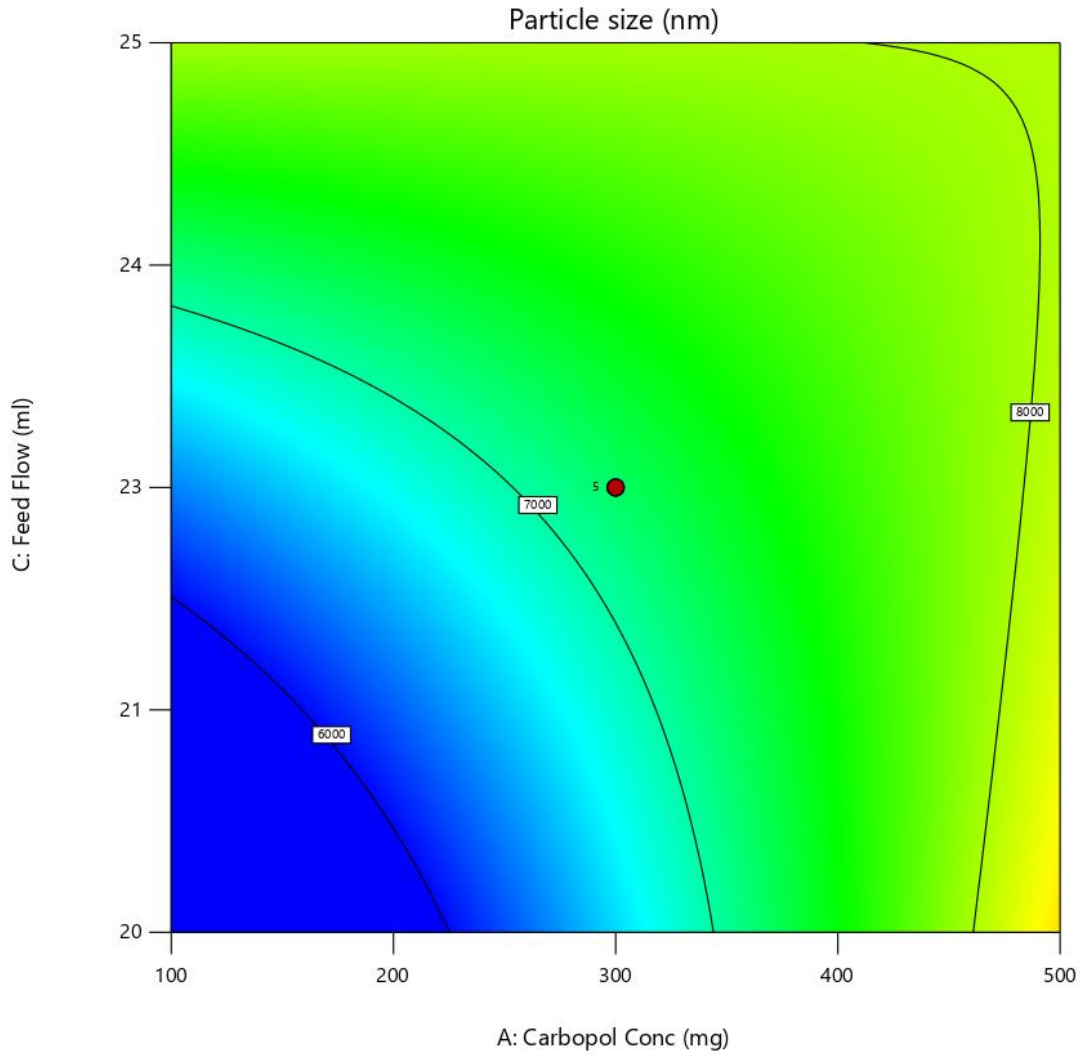


Figure 10 Contour Plots (2D) particle size, feed flow, and Carbopol conc. From the previous figure it is noticed when the Carbopol Conc increases from 100mg towards 500mg with an increase in feed flow from minimum to maximum, increase in particles was observed.

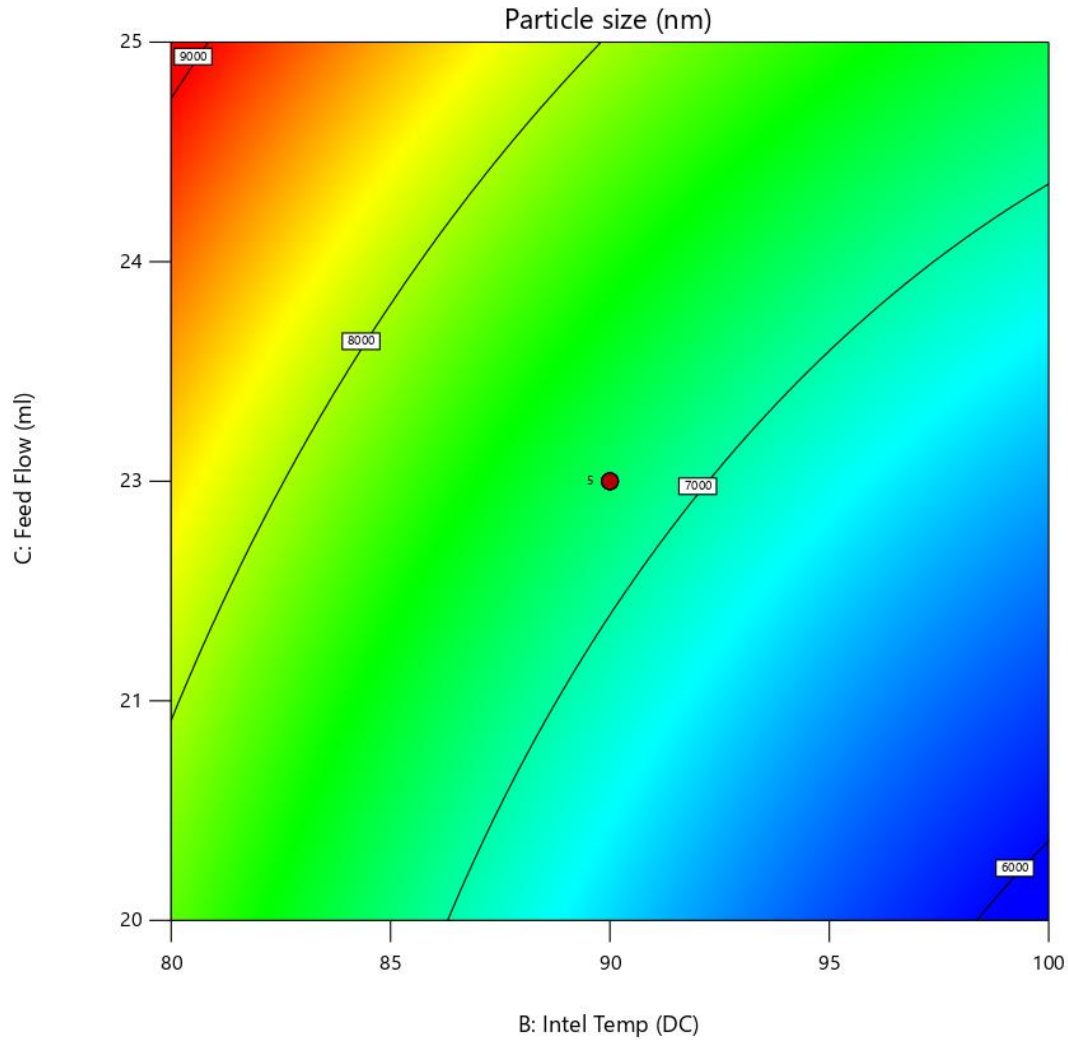


Figure 11 Contour Plots (2D) particle size, feed flow, and intel Temp.
 Analyzing the 2D contour plot of the effects of interaction on the particle size, big size of particles was observed when feed flow reached at highest 25ml with temperature in the range of 80°C to 85°C.

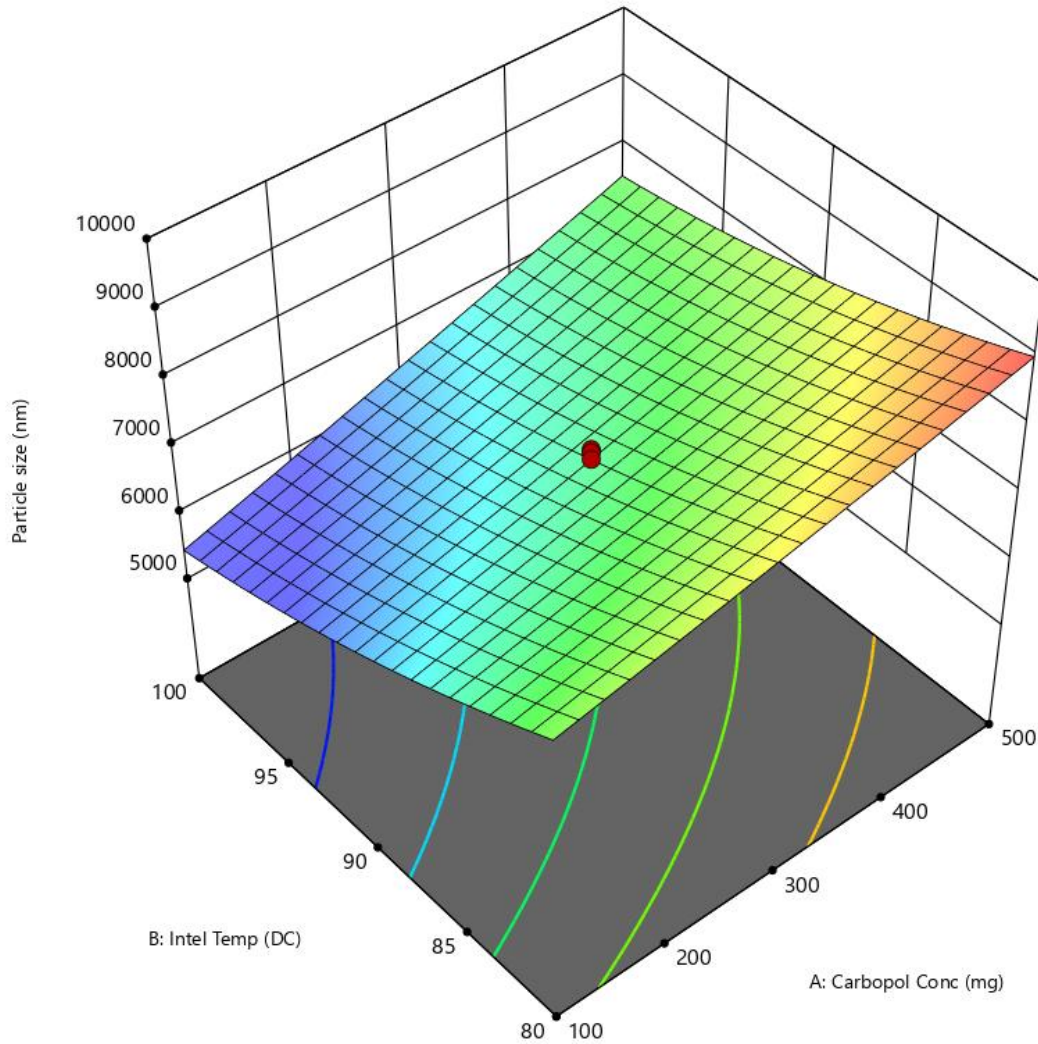


Figure 12: Contour Plots (3D) particle size, intel temp., and Carbopol conc.

Interpretation: (Effect of carbopol conc on particle size)

The interaction of the Carbopol Conc with the particle size is significant. It is observed that increasing the concentration of Carbopol results in increasing in size of the particles, this is due to more solid in a droplet may increase the size and also the droplet contains lesser amount to vaporize.

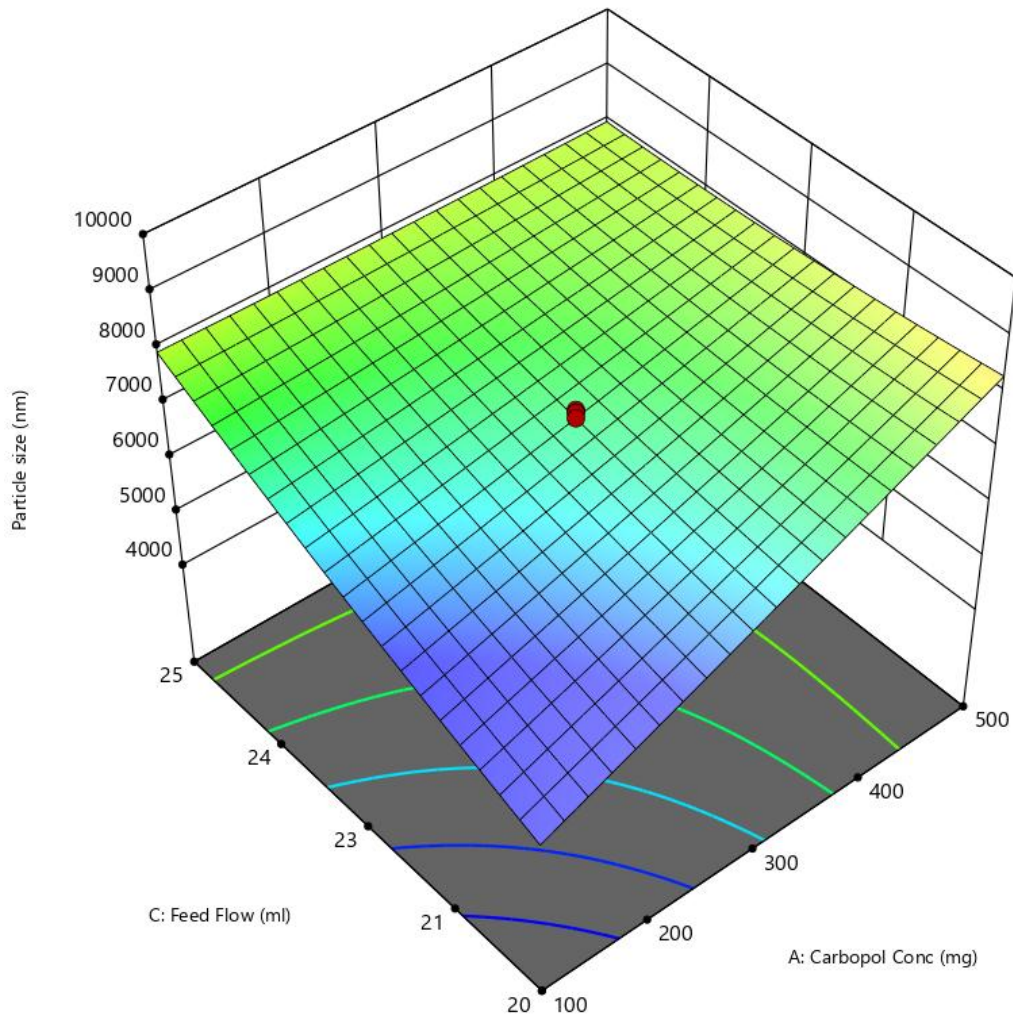


Figure 13: Contour Plots (3D) particle size, feed flow, and Carbopol conc.

Interpretation: (Effect of Feed flow on particle size)

The interaction of the Feed Flow with the particle size is significant. It is observed that with an increase in flow rate, increase in particle size.

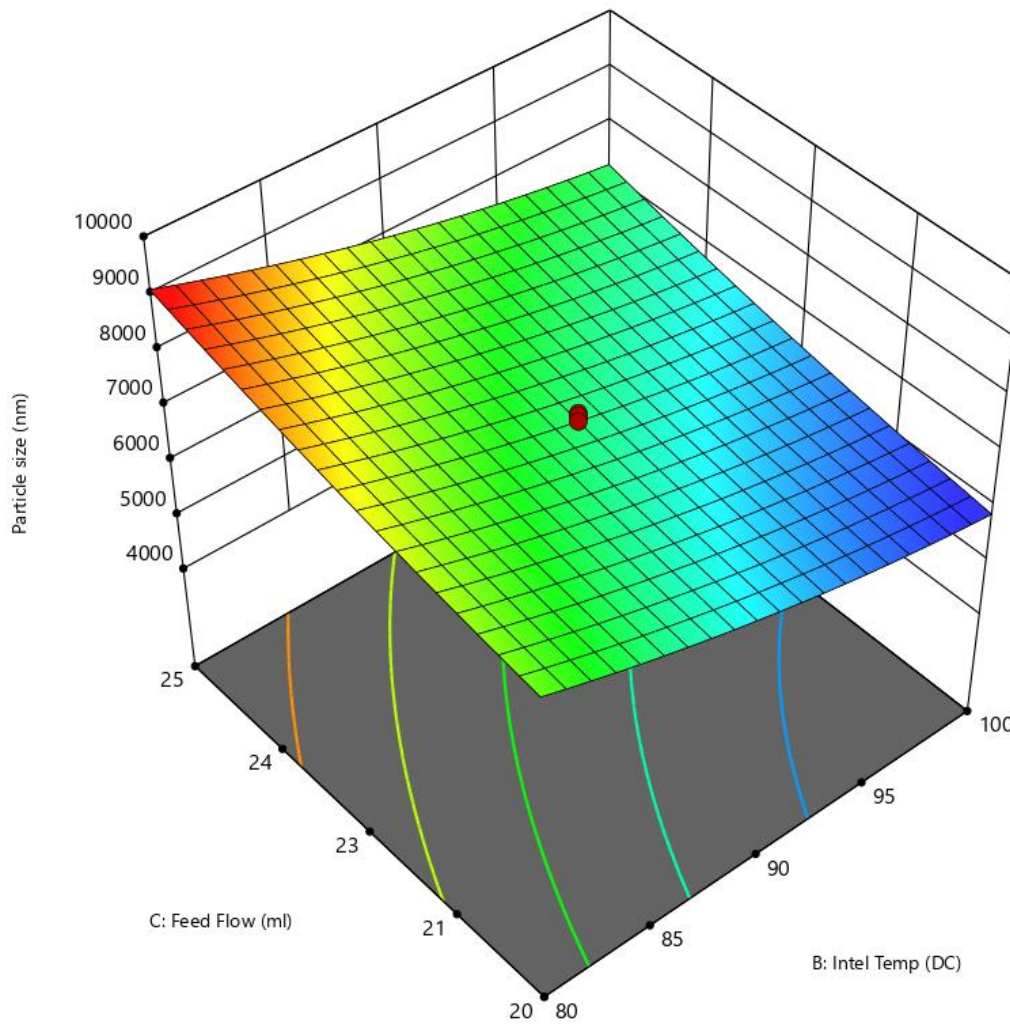


Figure 14 Contour Plots (3D) particle size, feed flow, and intel Temp.

Interpretation: (Effect of intel temp on particle size)

The interaction of the feed flow and particle size is significant. Surprisingly, an increase in inlet temperature shows a decrease in particle size.

Conclusion:

The Anova table for quadratic model shows, all three factors intel temp, carbopol conc. and feed flow are statistically significant for particle size (P-value<0.05). All three factors affect the size of particles in spray drying process. It is observed that particle size increases with feed flow and carbopol conc. also increases while intel temperature decreases.

4.7.Starting Points

Table 8: Number of Starting Points: 105

Carbopol	Intel	Feed	Predicted	Actual	Formulation
----------	-------	------	-----------	--------	-------------

Conc	Temp	Flow	Particle Size	Particle Size μm	Code
300	90	23	7322	7.302	CLSMO-1
105	83	23	7524	7.516	CLSMO-2
166	80	21	7544	7.552	CLSMO-3

CLSMO – Carbopol, linezolid, Microspheres, Spray Drying

From the previous table there three starting points with three formulation codes the first at Carbopol Conc. 300, intel Temp. 90, feed flow 23, predicted particle size 7322 and actual particle size μm 7.302 and its code is CLSMO-1

the second at Carbopol Conc. 105, intel Temp. 83, feed flow 23, predicted particle size 7524 and actual particle size μm 7.516 and its code is CLSMO-2

the last at Carbopol Conc. 166, intel Temp. 80, feed flow 21, predicted particle size 7544 and actual particle size μm 7.552 and its code is CLSMO-3.

Factor Coding: Actual

Particle size (nm)

Particle size (nm) = 7350
Std # 11 Run # 3

X1 = A: Carbopol Conc
X2 = B: Intel Temp
X3 = C: Feed Flow

Predicted values shown

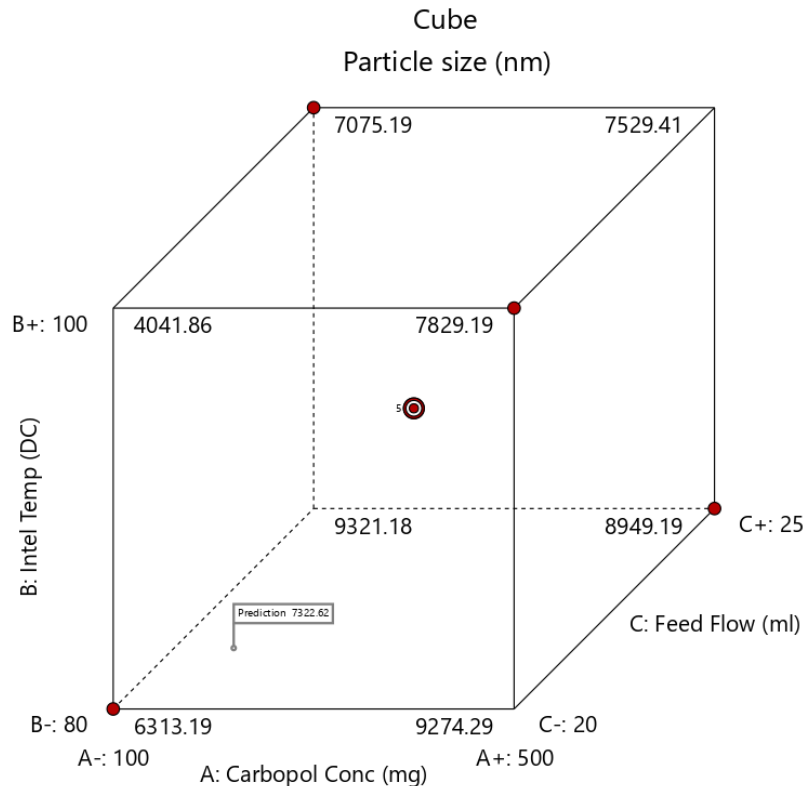


Figure 15: particle size in CLSMO-1 (a)

Factor Coding: Actual

Particle size (nm)
X1 = A: Carbopol Conc
X2 = B: Intel Temp
X3 = C: Feed Flow

Predicted values shown

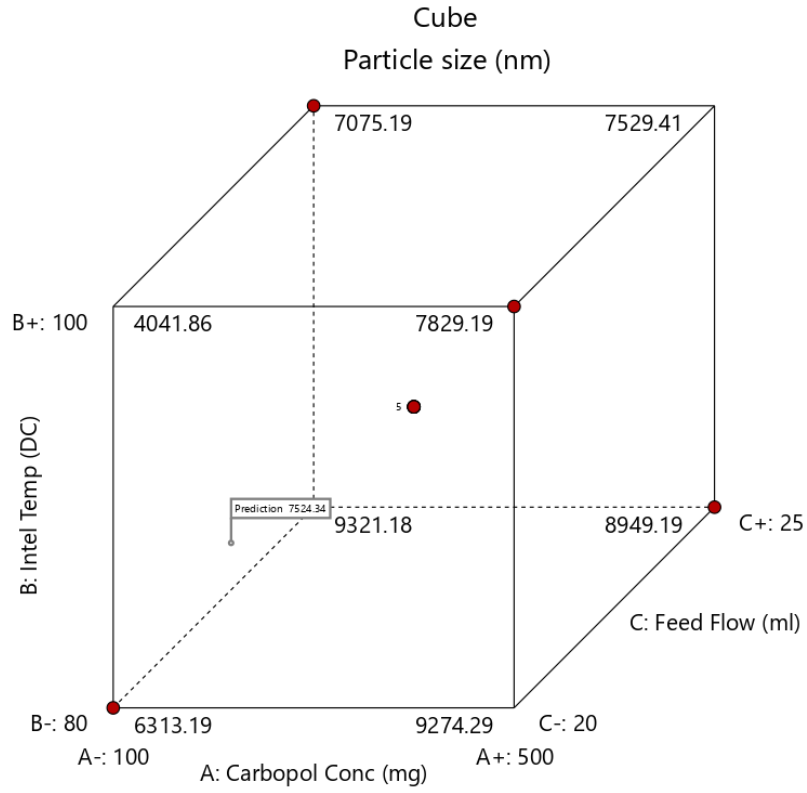


Figure 16: particle size in CLSMO-1 (b)

UNDER REVIEW

Factor Coding: Actual

Particle size (nm)
X1 = A: Carbopol Conc
X2 = B: Intel Temp
X3 = C: Feed Flow

Predicted values shown

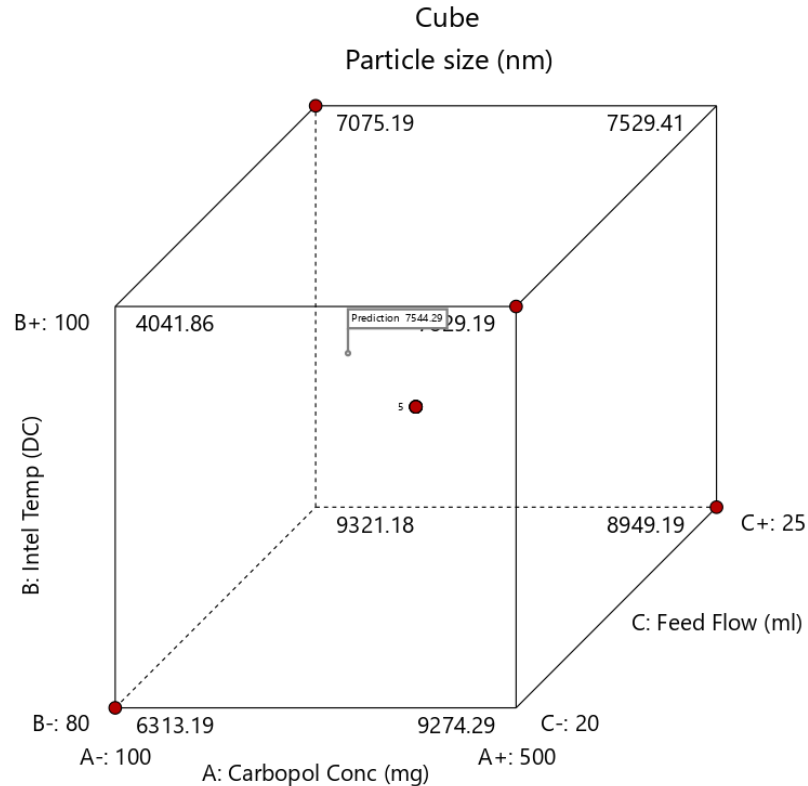


Figure 17: particle size in CLSMO-1 (c)

The results of the number optimization solution showed that three formulations were selected for further evaluation. The response for particle size was found to be similar to the response predicted by the design expert software. Following this, further studies were conducted using the best selected formulation code from the table.

4.8. Differential Scanning Calorimetry

The results obtained from the differential scanning calorimetry (DSC) analysis provided valuable insights into the thermal properties of the Linezolid, Carbopol, and CLSMO formulation. Importantly, no noticeable shift or alteration in the melting point was observed. This finding suggests that the presence of Carbopol and the encapsulation of Linezolid within the microspheres did not significantly affect the thermal behavior of the drug.

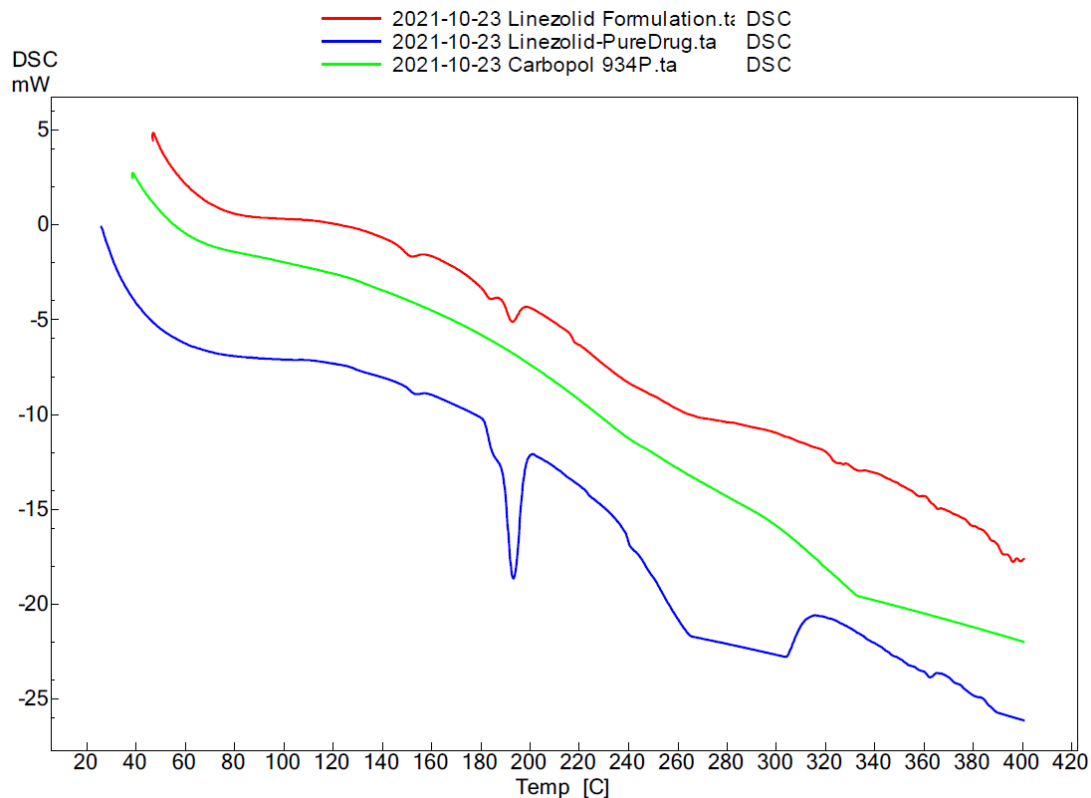


Figure 18: DSC of linezolid formulation, linezolid pure drug, and Carbopol

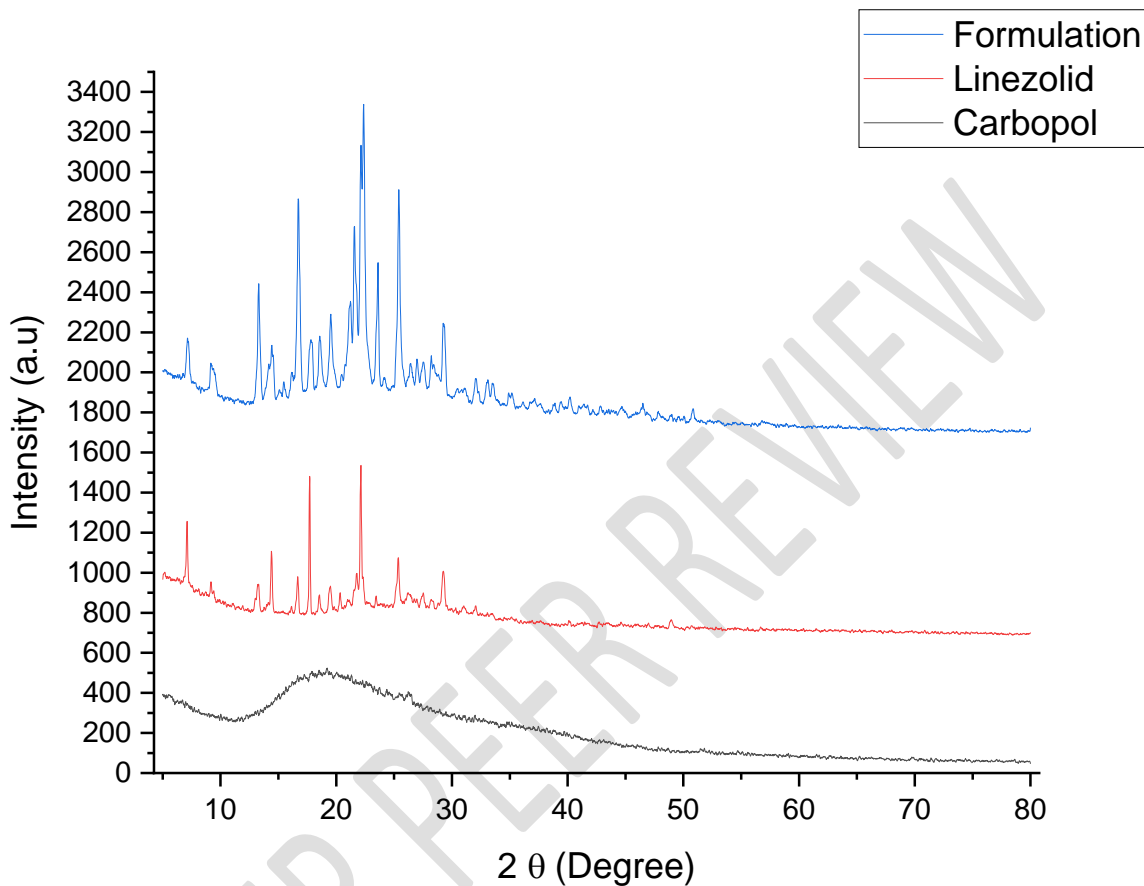
4.9.XRD studies

XRD analysis, way of the study of the crystal structure, is used to identify the crystalline phases present in a material and thereby reveal chemical composition information. Identification of phases is achieved by comparison of the acquired data to that in reference databases. In XRD analysis, a focused X-Ray beam is shot at the sample at a specific angle of incidence. The X-Rays deflect or "diffract" in various ways depending on the crystal structure (inter-atomic distances) of the sample. The locations (angles) and intensities of the diffracted X-Rays are measured.

X-ray diffraction analysis (XRD) is a technique used in materials science to determine the crystallographic structure of a material. XRD works by irradiating a material with incident X-rays and then measuring the intensities and scattering angles of the X-rays that leave the material

Present investigation of XRD studies qualitatively revealed the physical state and compatibility of the drug Linezolidin in the microsphere (MS) of Carbopol 934. In our investigation we chose two characteristics peaks at 2 Theta angles (14.40 and 22.12) observed in the XRD pattern of the pure Linezolidin were compared with its formulation in microsphere of Carbopol 934P.

The characteristics peaks of both the pure Linezolidin and its formulation in microsphere of Carbopol 934P were found to show similar XRD patterns but with different in their intensities as shown in the following figure



Both XRD pattern of pure Linezolidin and formulation in microsphere are characterized by the interplanar d-spacing, the intensities height (H) and area under the curve the peaks in the pattern as shown in the following tables.

The relative intensities heights of the characteristics peaks of our microsphere formulation were less than those of pure Linezolidin. It is cleared from results that there is a decrease in the crystalline peaks of Linezolidin in microsphere with increasing lattice spacing indicating that the drug has relatively become amorphous due to its dispersion in the amorphous region of semi crystalline polymeric microsphere of CLSMO at the molecular level.

Table 9: 2 Theta, Lattice spacing (\AA), Intensities (H) and Area under the curve the peaks in the Diffractogram of Linezolidin

Linezolid

2 Theta	Intensity (H)	Area under the curve	Lattice spacing (Å)
14.40749	275.38237	40.72298	6.15
22.12642	649.55377	120.49009	4.02

Table 10: 2 Theta, Lattice spacing (Å), Intensities (H) and Area under the curve the peaks in the Diffractogram of Linezolidin formulation in microsphere

Formulation in MS of Carbopol

2 Theta	Intensity (H)	Area under the curve	Lattice spacing (Å)
14.422	155.32681	47.81774	6.14
21.53483	486.83949	450.16384	4.13

4.10. Fourier-Transform Infra-Red (FT-IR)

Results: The FTIR spectral analysis of any drug molecule gives insight of the functional groups which can interact with drug carrier polymers and causes a shift in frequency and bandwidth of absorption peaks. Therefore, FTIR spectroscopy is one of important tools to find out the interactions and compatibility between the drug and polymers. The present investigation was carried out to prepare microspheres drug delivery system using linezolid antibiotic drug and carbopol 934p polymer.

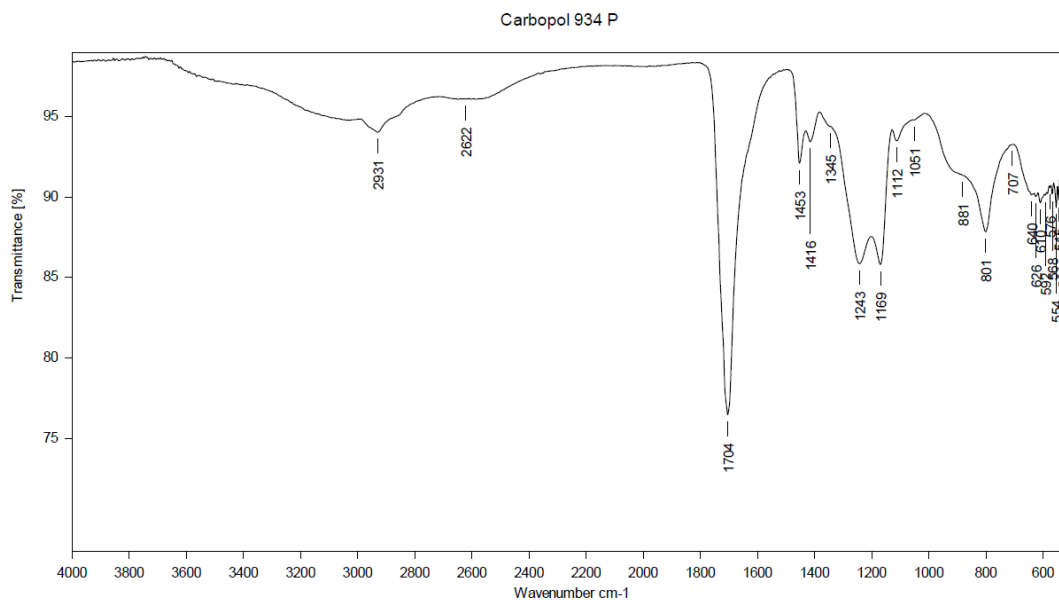


Figure 19: FTIR of carbopol 934P

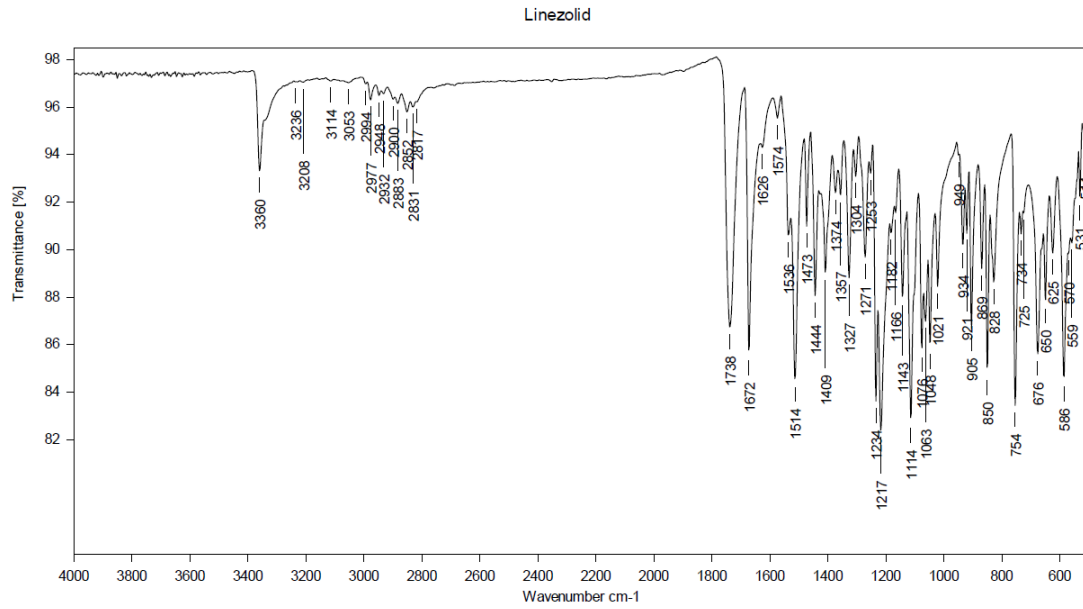


Figure 20: FTIR of Linezolid

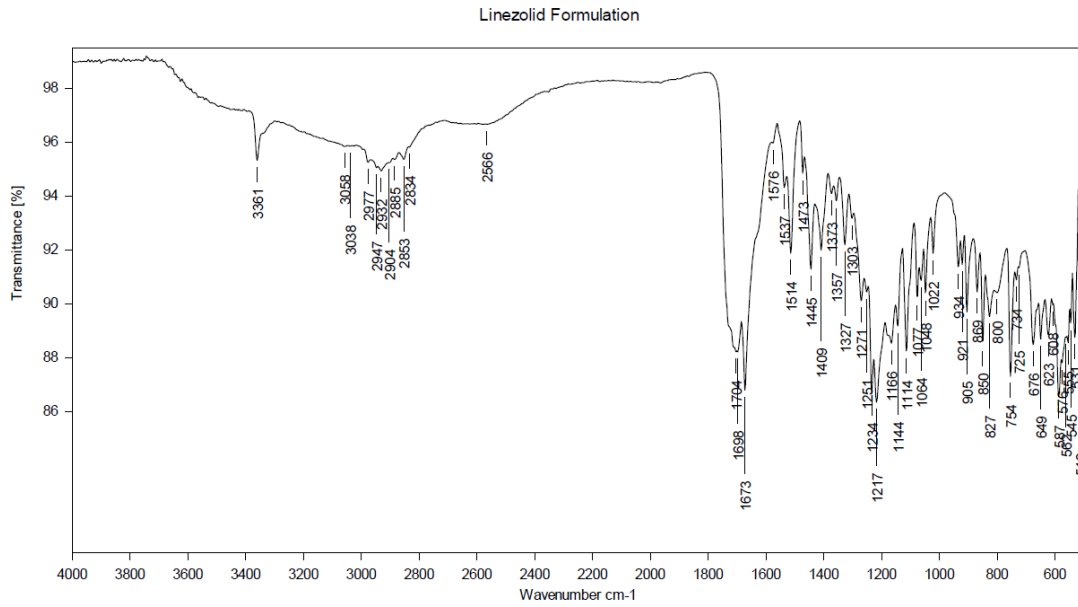
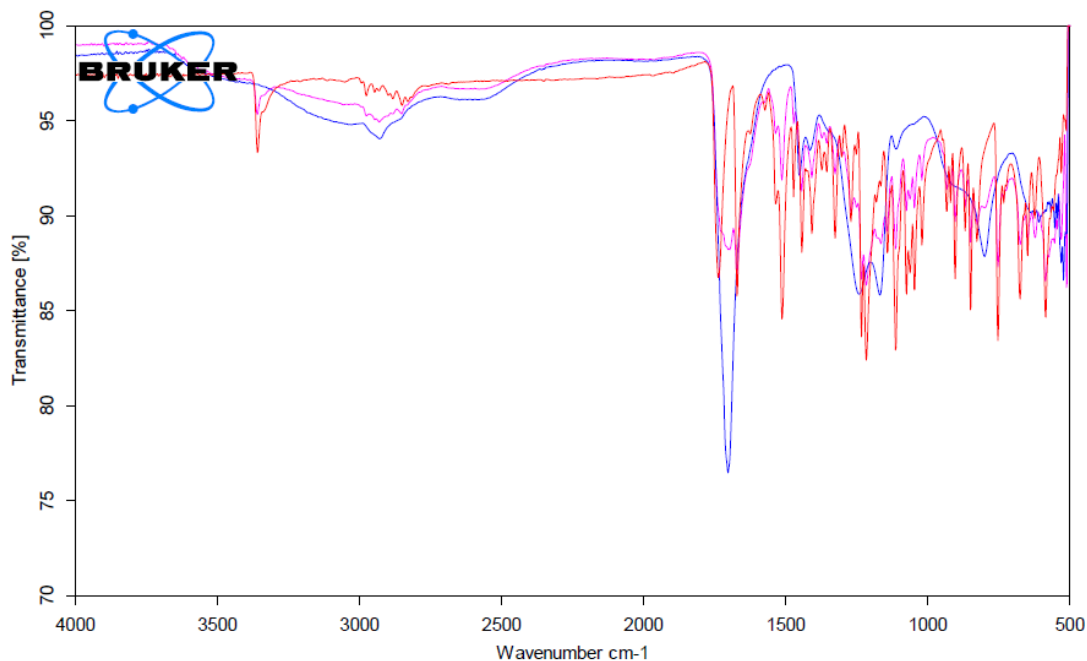


Figure 21: FTIR of Linezolid formulation



C:\PRL\Linezolid.0	Linezolid	Solid	10/19/2021
C:\PRL\Carbopol 934 P.0	Carbopol 934 P	Solid	10/19/2021
C:\PRL\Linezolid Formulation.0	Linezolid Formulation	Solid	10/19/2021

Page 1 of 1

Figure 22: FTIR of Linezolid formulation

Linezolid consists of 1, 3-oxazolidin-2-one bearing an N-3-fluoro-4-(morpholin-4-yl) phenyl group as well as an acetamidomethyl group at position 5. The IR spectra of linezolid along with the physical mixture of linezolid with carbopol 934p polymer are shown in the previous figures which displayed many intense, sharp absorption peaks that are due to the different functional groups present in the molecules. In the IR spectra of linezolid the wave number at 3360cm^{-1} and at 1672cm^{-1} showed the N-H stretching and N-H bending respectively. The wave number from 2817cm^{-1} to 2994cm^{-1} disclosed the presence C-H stretching and 1114cm^{-1} showed the ether functional group in morpholine moiety. The wave numbers of 1738cm^{-1} and 1672cm^{-1} are the characteristics absorption peaks which showed the presence of C=O stretching of an oxazolidinone carbonyl and C=O stretching of an acetamide carbonyl. The wave number at 1574cm^{-1} indicated the presence of C=C aromatic and the wave number 1409cm^{-1} corresponded the C-H scissoring & bending. The characteristics peaks of pure Linezolid at 3360 , 1672 , 2817 to 2994 , 1114 , 1738 and 1672cm^{-1} were also reported by other researcher in their study w0hich is almost similar to

peaks found in our study. Thus, indicating the identity and purity of the Linezolid drug. In IR spectra of carbopol 934p polymer has been presented. The recorded bands were found at 1704, 1169 and 1112 cm^{-1} wavenumbers due to the presence of carbonyl group. It has been observed in this analysis that Linezolid within microspheres of carbopol, drug-polymer physical mixture, contained the same peaks and preserved its individual peaks at the same wavenumbers as in its own spectrum. Similarly, no change in position of spectral peaks of carbopol polymer were observed before and after formulation. This investigation results suggest that there are no significant physical and chemical interactions between the functional groups of Linezolid and carbopol 934P polymer which ultimately form a stable blend.

4.11. In vitro release kinetics

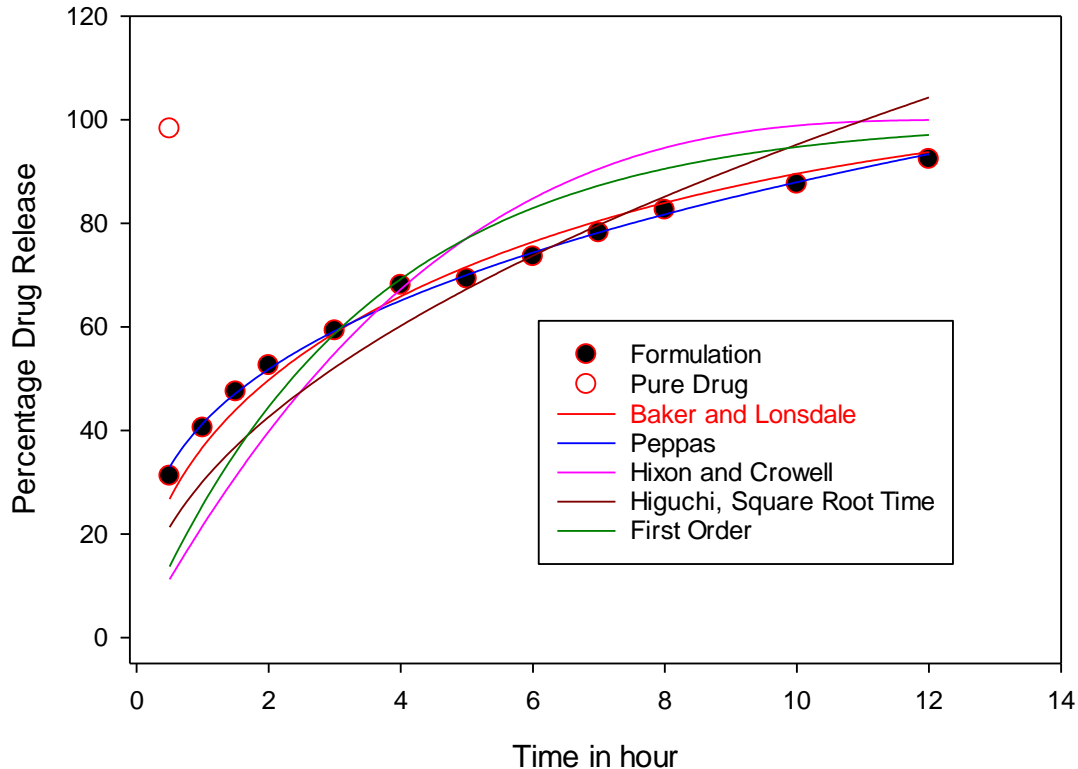


Figure 23: *in vitro* release kinetics

As shown in the above figure the pure drug released 100% in first hour and at the same time CLSMO drug released 30%. The efficacy of linezolid-containing Carbopol microspheres in drug delivery has been studied extensively. It has been found that the linezolid released 95.4% of the drug within the first half hour, while 22.11% of linezolid-containing Carbopol microspheres is released in the first half hour and the remaining drug is released completely (99.1%) within 12 hrs. This drug-release pattern

demonstrated an initial burst and is consistent with a biphasic model due to the loosely embedded drug on the particle surface. In the case of acute bacterial infections, the loading dose of 4–6 $\mu\text{g kg}^{-1}$ of linezolid is given intravenously over a 10-min period. Clinically, the initial burst release is important, as it acts as a loading dose, which helps to reach the minimum therapeutic concentration in the blood to show the drug's action. The release mechanism is studied by fitting the data to various kinetic models (SigmaPlot Ver 14.5) to understand the release mechanism, such as Baker and Lonsdale ($r^2=0.9789$), Peppas ($r^2=0.9960$), Hixon and Crowell ($r^2=0.5391$), Higuchi ($r^2=0.8175$), and First Order ($r^2=0.7300$). The regression square value of each of the five in vitro release kinetics - Baker and Lonsdale, Peppas, Hixon and Crowell, Higuchi, and First Order. The regression square value is a measure of how well the data fits the model, and a higher value indicates a better fit. The Peppas model had the highest regression square value of 0.9789.

The Baker and Lonsdale model had the highest regression square value of 0.9789, indicating that it had the best fit to the data. The Peppas model had a regression square value of 9960, indicating a very good fit. The Hixon and Crowell model had a regression square value of 5391, indicating a moderate fit. The Higuchi, Square Root model had a regression square value of 8175, indicating a good fit. Lastly, the First Order model had a regression square value of 0.7300, indicating a poor fit. The Peppas model assumes that the release of drug from a formulation is affected by the dissolution of the drug particles in a liquid medium. These findings are useful for the development of drug delivery systems for linezolid and other drugs.

CONCLUSION

In conclusion, the growing bacterial resistance to antimicrobial drugs has prompted researchers to explore novel treatment options. *Staphylococcus aureus*, a commonly encountered and potentially fatal bacteria, poses a significant challenge due to its resistance to many antibiotics. Linezolid, as the first therapeutically efficacious antibacterial oxazolidinone, has shown promise in combating drug-resistant bacteria, including *Staphylococcus aureus*. However, the frequent and chronic use of Linezolid can lead to adverse effects on non-target organs.

The development of Linezolid-loaded carbopol microspheres (CLSMO) is a significant achievement in delivering drugs to targeted areas of the body. The observed characteristics, such as the shriveled surface and average particle size, indicate the successful

formation of the microspheres. Additionally, the absence of significant physical and chemical interactions between Linezolid and the carbopol 934P polymer, as revealed by FTIR spectral analysis, ensures the stability of the formulation. Overall, the optimized formulation of Linezolid-loaded microspheres holds promise as an effective drug-delivery system, particularly for targeted delivery to the lungs. This innovation has the potential to mitigate the adverse effects associated with prolonged Linezolid usage, ultimately improving treatment outcomes. Future in vivo applications of this formulation may revolutionize the field of targeted drug delivery and contribute significantly to combating bacterial infections, thereby addressing the global challenge of antimicrobial resistance.

REFERENCES

1. Ferkol T, Schraufnagel D. The global burden of respiratory disease. *Annals of the American Thoracic Society*. 2014;11(3):404-6.
2. Whitehead L, Seaton P. The effectiveness of self-management mobile phone and tablet apps in long-term condition management: a systematic review. *Journal of medical Internet research*. 2016;18(5):e97.
3. Ramaiah B, Nagaraja SH, Kapanigowda UG, Boggarapu PR, Subramanian R. High azithromycin concentration in lungs by way of bovine serum albumin microspheres as targeted drug delivery: lung targeting efficiency in albino mice. *DARU Journal of Pharmaceutical Sciences*. 2016;24:1-11.
4. James SS, Bednarz B, Benedict S, Buchsbaum JC, Dewaraja Y, Frey E, et al. Current status of radiopharmaceutical therapy. *International Journal of Radiation Oncology* Biology* Physics*. 2021;109(4):891-901.
5. Hari SK, Gauba A, Shrivastava N, Tripathi RM, Jain SK, Pandey AK. Polymeric micelles and cancer therapy: An ingenious multimodal tumor-targeted drug delivery system. *Drug Delivery and Translational Research*. 2023;13(1):135-63.
6. Orowitz TE, Ana Sombo PPAA, Rahayu D, Hasanah AN. Microsphere polymers in molecular imprinting: Current and future perspectives. *Molecules*. 2020;25(14):3256.
7. Verma NK, Alam G, Vishwakarma D, Mishra J, Khan WU, Singh AP, et al. Recent Advances in Microspheres Technology for Drug Delivery.

International Journal of Pharmaceutical Sciences and Nanotechnology (IJPSN). 2015;8(2):2799-813.

8. Harsha NS. In vitro and in vivo evaluation of nanoparticles prepared by nano spray drying for stomach mucoadhesive drug delivery. *Drying Technology*. 2015;33(10):1199-209.
9. Santos-Rosales V, Iglesias-Mejuto A, García-González CA. Solvent-free approaches for the processing of scaffolds in regenerative medicine. *Polymers*. 2020;12(3):533.
10. SreeHarsha N, Venugopala KN, Nair AB, Roopashree TS, Attimarad M, Hiremath JG, et al. An efficient, lung-targeted, drug-delivery system to treat asthma via microparticles. *Drug design, development and therapy*. 2019:4389-403.
11. Chellappan DK, Yee LW, Xuan KY, Kunalan K, Rou LC, Jean LS, et al. Targeting neutrophils using novel drug delivery systems in chronic respiratory diseases. *Drug development research*. 2020;81(4):419-36.
12. Shankar P, Korukonda K, Bendre S, Behera D, Mirchandani L, Awad N, et al. Diagnoses and management of adult cough: an Indian Environmental Medical Association (EMA) position paper. *Respiratory Medicine*. 2020;168:105949.
13. Li J, Zhou Z, Liu X, Zheng Y, Li C, Cui Z, et al. Material-herbology: An effective and safe strategy to eradicate lethal viral-bacterial pneumonia. *Matter*. 2021;4(9):3030-48.
14. Gupta S, Kumar S. An overview on intranasal drug delivery system: recent technique and its contribution in therapeutic management. *Current Research in Pharmaceutical Sciences*. 2019.
15. Chandrasekhar A, Kim C-S, Naji M, Natarajan K, Hahn J-O, Mukkamala R. Smartphone-based blood pressure monitoring via the oscillometric finger-pressing method. *Science translational medicine*. 2018;10(431):eaap8674.
16. Peloquin CA, Davies GR. The treatment of tuberculosis. *Clinical Pharmacology & Therapeutics*. 2021;110(6):1455-66.
17. Sehgal I, Dhooria S, Choudhary H, Aggarwal A, Garg M, Chakrabarti A, et al. Monitoring treatment response in chronic pulmonary aspergillosis: role of clinical, spirometric and immunological markers. *Clinical Microbiology and Infection*. 2019;25(9):1157. e1-. e7.
18. AKDAĞ ÇAYLI Y. Development of dry powder inhaler formulations for drug delivery systems. *Journal of research in pharmacy*. 2019;23(6).

19. Nsairat H, Khater D, Sayed U, Odeh F, Al Bawab A, Alshaer W. Liposomes: structure, composition, types, and clinical applications. *Heliyon*. 2022;8(5):e09394.
20. Murthy SK. Nanoparticles in modern medicine: state of the art and future challenges. *International journal of nanomedicine*. 2007;2(2):129-41.
21. Jain NK, Gupta U. Application of dendrimer–drug complexation in the enhancement of drug solubility and bioavailability. *Expert opinion on drug metabolism & toxicology*. 2008;4(8):1035-52.
22. Wolinsky JB, Grinstaff MW. Therapeutic and diagnostic applications of dendrimers for cancer treatment. *Advanced drug delivery reviews*. 2008;60(9):1037-55.
23. Claire du Toit L, Pillay V, Choonara YE, Pillay S, Harilall S-I. Patenting of nanopharmaceuticals in drug delivery: no small issue. *Recent patents on drug delivery & formulation*. 2007;1(2):131-42.
24. Wong HL, Bendayan R, Rauth AM, Li Y, Wu XY. Chemotherapy with anticancer drugs encapsulated in solid lipid nanoparticles. *Advanced drug delivery reviews*. 2007;59(6):491-504.
25. Jain K. Use of nanoparticles for drug delivery in glioblastoma multiforme. *Expert review of neurotherapeutics*. 2007;7(4):363-72.
26. Marcato PD, Durán N. New aspects of nanopharmaceutical delivery systems. *Journal of nanoscience and nanotechnology*. 2008;8(5):2216-29.
27. Pridgen EM, Langer R, Farokhzad OC. Biodegradable, polymeric nanoparticle delivery systems for cancer therapy. 2007.
28. Tour JM. Nanotechnology: the passive, active and hybrid sides—gauging the investment landscape from the technology perspective. *Nanotech L & Bus*. 2007;4:361.
29. Singh A, Dutta MK, ParthaSarathi M, Uher V, Burget R. Image processing based automatic diagnosis of glaucoma using wavelet features of segmented optic disc from fundus image. *Computer methods and programs in biomedicine*. 2016;124:108-20.
30. Sohail MF, Rehman M, Sarwar HS, Naveed S, Salman O, Bukhari NI, et al. Advancements in the oral delivery of Docetaxel: challenges, current state-of-the-art and future trends. *International journal of nanomedicine*. 2018;13:3145.
31. Sharma D, Singh M, Kumar P, Vikram V, Mishra N. Development and characterization of morin hydrate loaded microemulsion for the

management of Alzheimer's disease. *Artificial cells, nanomedicine, and biotechnology*. 2017;45(8):1620-30.

32. Lingayat VJ, Zarekar NS, Shendge RS. Solid lipid nanoparticles: a review. *Nanoscience and Nanotechnology Research*. 2017;4(2):67-72.

33. Padhi S, Hassan N, Jain P, Singh M, Mohapatra S, Iqbal Z. Microparticles, Microspheres, and Microemulsions as Pulmonary Drug Delivery Systems for the Treatment of Respiratory Diseases. *Advanced Drug Delivery Strategies for Targeting Chronic Inflammatory Lung Diseases*: Springer; 2022. p. 281-302.

34. Mal A, Bag S, Ghosh S, Moulik SP. Physicochemistry of CTAB-SDS interacted cationic micelle-vesicle forming system: An extended exploration. *Colloids and Surfaces A: Physicochemical and Engineering Aspects*. 2018;553:633-44.

35. A Dobrovolskaia M. Dendrimers effects on the immune system: insights into toxicity and therapeutic utility. *Current pharmaceutical design*. 2017;23(21):3134-41.

36. Kocks JW, Chrystyn H, Van Der Palen J, Thomas M, Yates L, Landis SH, et al. Systematic review of association between critical errors in inhalation and health outcomes in asthma and COPD. *NPJ primary care respiratory medicine*. 2018;28(1):43.

37. Hardainyan S, Kumar K, Nandy BC, Saxena R. Design, formulation and in vitro drug release from transdermal patches containing imipramine hydrochloride as model drug. *Int J Pharm Pharm Sci*. 2017;9:220-5.

38. Mandal A, Bisht R, Rupenthal ID, Mitra AK. Polymeric micelles for ocular drug delivery: From structural frameworks to recent preclinical studies. *Journal of Controlled Release*. 2017;248:96-116.